

Effective cutting of a quantum spin chain by bond impurities

T. J. G. Apollaro,^{1,2} F. Plastina,¹ L. Bianchi,^{3,4} A. Cuccoli,^{5,6} R. Vaia,^{6,7} P. Verrucchi,^{5,6,7} and M. Paternostro^{2,8}

¹*Dipartimento di Fisica & INFN–Gruppo collegato di Cosenza, Università della Calabria, Via P. Bucci, 87036 Arcavacata di Rende (CS), Italy*

²*Centre for Theoretical Atomic, Molecular, and Optical Physics, School of Mathematics and Physics, Queen’s University Belfast, BT7 1NN, United Kingdom*

³*Department of Physics and Astronomy, University College London, Gower St., London WC1E 6BT, United Kingdom*

⁴*ISI Foundation, Via Alassio 11/c, I-10126 Torino (TO), Italy*

⁵*Dipartimento di Fisica, Università di Firenze, Via G. Sansone 1, I-50019 Sesto Fiorentino (FI), Italy*

⁶*INFN Sezione di Firenze, via G. Sansone 1, I-50019 Sesto Fiorentino (FI), Italy*

⁷*Istituto dei Sistemi Complessi, Consiglio Nazionale delle Ricerche, via Madonna del Piano 10, I-50019 Sesto Fiorentino (FI), Italy*

⁸*Institut für Theoretische Physik, Albert-Einstein-Allee 11, Universität Ulm, D-89069 Ulm, Germany*

(Received 26 September 2013; published 27 November 2013)

Spin chains are promising media for short-haul quantum communication. Their usefulness is manifested in all those situations where stationary information carriers are involved. In the majority of the communication schemes relying on quantum spin chains, the latter are assumed to be finite in length, with well-addressable end-chain spins. In this paper we propose that such a configuration could actually be achieved by a mechanism that is able to effectively cut a spin ring through the insertion of bond defects. We then show how suitable physical quantities can be identified as figures of merit for the effectiveness of the cut. We find that, even for modest strengths of the bond defect, a ring is effectively cut at the defect site. In turn, this has important effects on the amount of correlations shared by the spins across the resulting chain, which we study by means of a scattering-based mechanism of a clear physical interpretation.

DOI: [10.1103/PhysRevA.88.052336](https://doi.org/10.1103/PhysRevA.88.052336)

PACS number(s): 03.67.Hk, 75.10.Pq, 75.30.Hx

I. INTRODUCTION

In the past decade, the idea of connecting stationary information carriers via one-dimensional spin systems has been developed significantly and several strategies have been proposed for obtaining high-quality quantum-state and entanglement transfer, as well as entangling gates [1,2]. The general paradigm involves two remote qubits located at each end of a chain of interacting spins mediating the exchange of information between the distant particles. Together with the strength of the intrachain coupling, the length of the chain, as measured for instance by the number of its spins, is a key parameter that determines the operational time and quality of a given communication scheme. In fact, in any practical implementation, the spin-chain medium needs to be of finite length with well-identified and -addressable first (*head*) and last (*tail*) elements.

Depending on the actual physical realization, one can think of different ways of fulfilling such requirements. In this paper we consider the case of a medium modelled by a chain of interacting spin-1/2 particles, such as the crystals listed in Table 1 of Ref. [3] or the more recently proposed molecular rings [4,5]. Other physical realizations, ranging from ultracold-atom systems to coupled-cavity arrays [6,7], adhere well to such a model. We specifically address the problem of obtaining a one-dimensional spin system of finite length and open boundary conditions (OBC), hereafter called “segment,” out of a spin chain with periodic boundary conditions (PBC). As the latter structure can be generally represented as a closed ring (of either finite or infinite length), we will refer to the above problem as that of “cutting a ring.”

As a ring-cutting mechanism basically changes PBC into OBC, and relying on general arguments about how impurities

affect the behavior of one-dimensional systems, we propose the insertion of one impurity as an effective tool for realizing one cut. In particular, we consider the case when the impurity corresponds to a variation of the interaction strength between two neighboring spins, with respect to the otherwise homogeneous couplings. The effect of the presence of this kind of bond impurity on the ground state of the antiferromagnetic XXZ Heisenberg spin- $\frac{1}{2}$ model has been investigated via renormalization group techniques in Refs. [8–10], where it has been shown that this kind of impurity embodies a relevant perturbation and yields to a fixed point in the renormalization-group flow corresponding to OBC for an infinite interaction’s strength. In this paper we solve analytically the impurity XX Heisenberg spin- $\frac{1}{2}$ model via the Jordan-Wigner mapping into a noninteracting spinless fermionic model and determine quantitatively the cutting effect for finite interaction’s strength via quantum-information-inspired figures of merit, such as classical and quantum correlations and fidelity measures.

An equally important motivation to investigate the impurity-driven ring-cutting mechanism is to analyze the emergence of boundary effects, such as Friedel-like oscillations [11] of the fermion density, i.e., the local magnetization, driven by the impurity strength. These effects are more pronounced in proximity of the impurity spins [12–14]. They allow for the tuning of the degree of entanglement shared by two arbitrary spins of the medium (even different from the impurities) along the lines of Refs. [15–18].

The paper is organized as follows: In Sec. II we introduce the specific model addressed here, namely that of a ring of $2M$ spin-1/2 particles, interacting via a nearest-neighbor, planar, and isotropic magnetic exchange model, hereafter referred to as XX interaction. The effect of an inserted bond impurity is

here analytically studied in the thermodynamic limit $M \rightarrow \infty$. In Sec. III we discuss the thermodynamic-limit behavior of in- and out-of-plane magnetic correlations, concurrence [19], and quantum discord [20–22], which are some of our elected figures of merit for the characterization of the ring-cutting mechanism. The case of finite M is considered in Sec. IV, where we study the fidelity [23] between the ground state of a ring that has been effectively cut by a bond impurity and that of the segment it should mimic. The overall analysis is carried out as the parameter characterizing the bond impurity is varied and, as far as the finite-length case is concerned, for different values of M . Finally, we draw our conclusions in Sec. V.

II. THE MODEL

We consider a one-dimensional system of $2M$ ($M \in \mathbb{N}$) interacting spin-1/2 particles in the presence of a uniform magnetic field. The interaction is of the isotropic and planar (XX) Heisenberg form

$$\hat{\mathcal{H}}_0 = -\frac{J}{2} \sum_{n=-M+\frac{1}{2}}^{M-\frac{1}{2}} (\hat{\sigma}_n^x \hat{\sigma}_{n+1}^x + \hat{\sigma}_n^y \hat{\sigma}_{n+1}^y + 2h \hat{\sigma}_n^z), \quad (1)$$

where $(\hat{\sigma}_n^x, \hat{\sigma}_n^y, \hat{\sigma}_n^z)$ are the Pauli matrices for the spin at site n , J is the homogeneous coupling, and h is the magnetic field. The $2M$ lattice sites are labelled by the half-integer index $n = -M + \frac{1}{2}, \dots, M - \frac{1}{2}$. Correspondingly, the lattice bonds are labeled by the integer index $b = -M + 1, \dots, M$, with $b = n + 1/2$ indicating the bond between sites $n - 1$ and n . This notation allows the reflection symmetry with respect to the impurity bond to emerge more clearly in many of the following equations involving the correlation functions which, on the other hand, refer to lattice sites. The enforcement of the PBC conditions $\hat{\sigma}_{M+n} = \hat{\sigma}_{-M+n}$ makes Eq. (1) the Hamiltonian of a ring.

We introduce a single bond impurity (BI) by varying the exchange integral that generates the bond $b = 0$, i.e., the interaction strength between the two spins on sites $n = -\frac{1}{2}$ and $n = \frac{1}{2}$ (which we will refer to as the impurity spins). This implies adding the term

$$\hat{\mathcal{H}}_1 = \frac{J-j}{2} (\hat{\sigma}_{-\frac{1}{2}}^x \hat{\sigma}_{\frac{1}{2}}^x + \hat{\sigma}_{-\frac{1}{2}}^y \hat{\sigma}_{\frac{1}{2}}^y) \quad (2)$$

to the translation-invariant Hamiltonian in Eq. (1). Throughout the rest of the paper, we assume $J = 1$ as the energy unit. The resulting system $\hat{\mathcal{H}} = \hat{\mathcal{H}}_0 + \hat{\mathcal{H}}_1$ is illustrated in Fig. 1, where j gives the coupling strength and $j = 1$ ($j = 0$) corresponds to the well-known $2M$ -PBC ($2M$ -OBC) spin chains [24]. For every value that differs from the two cases above, we diagonalize the Hamiltonian as follows.

The total Hamiltonian $\hat{\mathcal{H}}_0 + \hat{\mathcal{H}}_1$ can be mapped via the Jordan-Wigner transformation [24] into

$$\begin{aligned} \hat{\mathcal{H}} = & - \sum_{n=-M+\frac{1}{2}}^{M-\frac{1}{2}} (\hat{c}_{n+1}^\dagger \hat{c}_n + \text{H.c.} + 2h \hat{c}_n^\dagger \hat{c}_n) \\ & - (j-1) \left(\hat{c}_{\frac{1}{2}}^\dagger \hat{c}_{-\frac{1}{2}} + \text{H.c.} \right), \end{aligned} \quad (3)$$

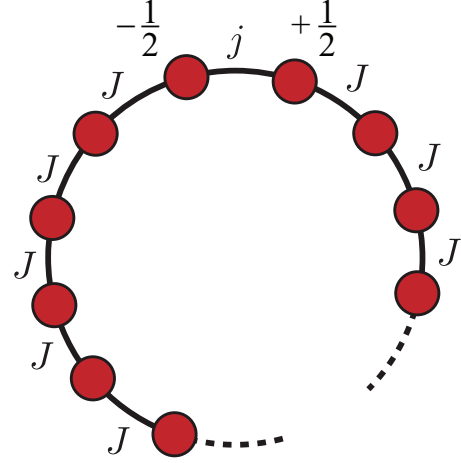


FIG. 1. (Color online) A ring of interacting spin-1/2 particles, all coupled through an XX model, includes a bond defect: While all spin pairs $(n, n+1)$ with $n \neq -1/2$ are mutually interacting with strength J , the pair $(-1/2, 1/2)$ experiences the strength j . The spins are all subjected to a homogeneous magnetic field h .

where $\{c_n, c_n^\dagger\}$ are the fermionic destruction and creation operators. As translation symmetry is broken for $j \neq 1$, a Fourier transform does not diagonalize Eq. (3). It is nevertheless possible to solve the model analytically by making use of a Green function approach [25,26]. The key steps of this procedure are outlined in Appendix A and the diagonalized Hamiltonian in the thermodynamic limit finally reads

$$\hat{\mathcal{H}} = \int_{-\pi}^{\pi} \frac{dk}{2\pi} E_k \hat{\zeta}_k^\dagger \hat{\zeta}_k + E_+ \hat{\zeta}_+^\dagger \hat{\zeta}_+ + E_- \hat{\zeta}_-^\dagger \hat{\zeta}_-. \quad (4)$$

The first term represents the intraband contributions and we have introduced the operators

$$\hat{\zeta}_k = \frac{1}{\sqrt{2M}} \sum_n e^{-ikn} (1 + f_{kn}) \hat{c}_n, \quad (5)$$

which annihilate fermions with energy $E_k = 2(\cos k - h)$. Here, the functions f_{kn} account for the spatial distortion of the intraband excitations as

$$f_{kn} = \begin{cases} \frac{i(j^2-1)e^{2ikn}}{2 \sin |k| - i(j^2-1)e^{i|k|}} & \text{if } kn > 0 \\ \frac{2(j-1) \sin |k| + i(j^2-1)e^{i|k|}}{2 \sin |k| - i(j^2-1)e^{i|k|}} & \text{if } kn < 0 \end{cases}. \quad (6)$$

Such distortion is evidently due to the BI ($f_{kn} = 0$ for $j = 1$) and is responsible for the oscillations observed in the correlations, as discussed in the following section. The second term of Eq. (4) accounts for two discrete-energy eigenstates E_\pm which appear only for $j > 1$; their energies are $E_\pm = -2h \pm (j+1/j)$, above and below the band, respectively. They correspond to excitations that, once expressed in terms of direct lattice-site fermionic operators, take the form

$$\hat{\zeta}_\pm = \sqrt{\sinh q} \sum_n (\pm)^{n+\frac{1}{2}} e^{-q|n|} \hat{c}_n, \quad (7)$$

with $q = \ln j$ being the reciprocal of the localization length.

Let us now compare the behavior of the system in the two extreme cases of $j = 0$ and $j \rightarrow \infty$. First, one can easily see that for $kn < 0$ in both cases one has $f_{kn} = -1$, namely the impurity acts as a purely reflective barrier yielding complete

backscattering. On the other hand, for $kn > 0$ the distortions of the in-band excitations in the two limits read $f_{kn} = -e^{i(2kn \pm |k|)}$, respectively. It follows that for $j \rightarrow \infty$ the distortion at the impurity sites is $f_{k, \frac{1}{2}} = f_{k, -\frac{1}{2}} = -1$, meaning that these sites completely decouple from the rest of the system, their state being exclusively determined by the two, now completely localized, out-of-band states $|E_{\pm}\rangle = \frac{1}{\sqrt{2}}(c_{\frac{1}{2}}^{\dagger} \mp c_{-\frac{1}{2}}^{\dagger})|0\rangle$; as they do not take part in the dynamics, the spins at sites $n = \pm 3/2$ take the role of head and tail of a segment of length $2M - 2$. Of course, for $j = 0$ the resulting segment has length $2M$. This argument suggests that one BI can indeed change the boundary conditions from PBC to OBC. In other terms, a segment can be obtained not only by actually cutting the ring ($j = 0$) but also by making the interaction between the spins sitting at sites $n = \pm 1/2$ strong enough with respect to the coupling between all the other nearest-neighbor spins ($j \gg 1$), as to effectively decouple them from the rest of the system.

In the next section we further explore this idea in the case $M \rightarrow \infty$, where the availability of the analytical results presented here allows us, through a straightforward application of Wick's theorem [24], to exactly evaluate two-points correlations functions, concurrence and quantum discord [20–22]. We focus on the possibility that the efficiency of the ring-cutting mechanism described above holds for moderately large values of j .

III. EFFECTIVE RING-CUTTING MECHANISM: STUDY OF THE TWO-POINT FUNCTIONS

In this section we study the effects of the BI on two-point functions, i.e., quantities relative to spin pairs. As far as we only consider pairs of nearest-neighbor spins, such quantities can be labelled by the integer bond-index b representing the distance in lattice spacings from the BI, according to $O_{n,n+1} = O_b$ with $b = n + 1/2$. We first analyze the nearest-neighbor magnetic correlations $g_b^{\alpha,\alpha} \equiv \langle \sigma_n^{\alpha} \sigma_{n+1}^{\alpha} \rangle$ ($\alpha = x, z$). For any $j \neq 1$, Friedel-like oscillations appear and induce a spatial modulation of the correlations with periodicity $p = \pi/k_F$, where $k_F = \cos^{-1} h$ is the Fermi momentum. In Fig. 2 we consider $h = 0$, corresponding to $p = 2$, and study $g_b^{\alpha,\alpha}$ against the value of b for various choices of j . The presence of the BI modifies the strength of correlations and the following relations (b is an integer) clearly emerge:

$$\begin{aligned} |g_{2b}^{\alpha,\alpha}(j < 1)| &< |g^{\alpha,\alpha}(j = 1)| < |g_{2b}^{\alpha,\alpha}(j > 1)|, \\ |g_{2b+1}^{\alpha,\alpha}(j < 1)| &> |g^{\alpha,\alpha}(j = 1)| > |g_{2b+1}^{\alpha,\alpha}(j > 1)|, \end{aligned} \quad (8)$$

where the bond-index dependence is omitted for $j = 1$, as in the uniform case PBC guarantee translation invariance. From the above inequalities we deduce that the results corresponding to the limit $j \rightarrow \infty$ cannot be possibly related with the behavior of the segment obtained by an actual cut, i.e., what is found by setting $j = 0$. Indeed, $g_b^{\alpha,\alpha}(\infty)$ in general differs from $g_b^{\alpha,\alpha}(0)$. In fact, as already mentioned at the end of the above section, we expect the $j \rightarrow \infty$ limit to reproduce the behavior of a segment with head and tail at $n = \pm 3/2$, i.e., $b = \pm 2$. Therefore, in all those cases for which the actual value of M is not relevant, such as in the thermodynamic limit considered here, the meaningful comparison to be performed involves $g_b^{\alpha,\alpha}(j = 0)$ and $g_{b+1}^{\alpha,\alpha}(j \rightarrow \infty)$. In order to quantitatively

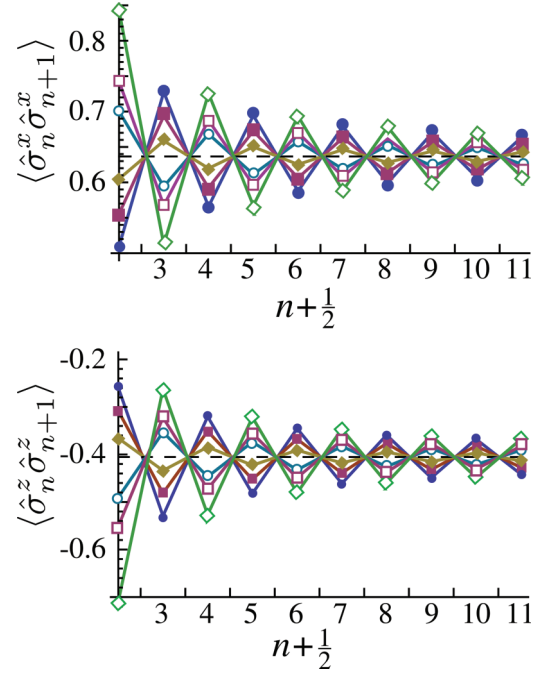


FIG. 2. (Color online) Correlators $\langle \hat{\sigma}_n^x \hat{\sigma}_{n+1}^x \rangle$ (top) and $\langle \hat{\sigma}_n^z \hat{\sigma}_{n+1}^z \rangle$ (bottom) for $j = 0, 0.5, 0.8, 1.5, 2, 11$ (corresponding to increasing absolute values for $n+1/2$ even). The straight lines correspond to the correlators in the PBC case, $j = 1$. For $j = 11$ the data are indistinguishable from the OBC limit.

check to what extent a model with large j can be actually considered to behave as a segment, in Fig. 3 we compare $g_2^{\alpha,\alpha}$ and $g_3^{\alpha,\alpha}$ for increasing values of j . Clearly, the correlations along x and z almost match the values corresponding to a true segment already for $j > 8$, confirming that an effective ring-cutting mechanism takes place.

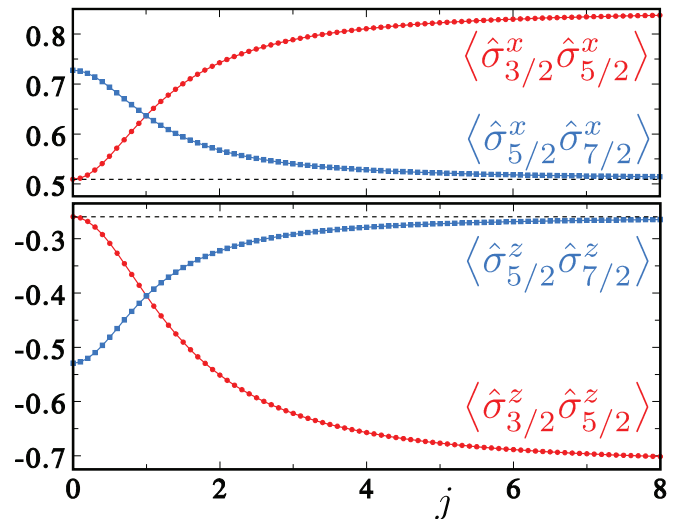


FIG. 3. (Color online) The nearest-neighbor correlation functions $\langle \hat{\sigma}_n^x \hat{\sigma}_{n+1}^x \rangle$ and $\langle \hat{\sigma}_n^z \hat{\sigma}_{n+1}^z \rangle$ corresponding to the second and third bond after the defect, vs j . The xx (zz) correlators take positive (negative) values; their absolute value increases (decreases) with j for $n = 3/2$ ($n = 5/2$). The dashed lines show that the third-bond correlators at $j \rightarrow \infty$ behave as the second-bond correlators of the open chain, i.e., $j = 0$.

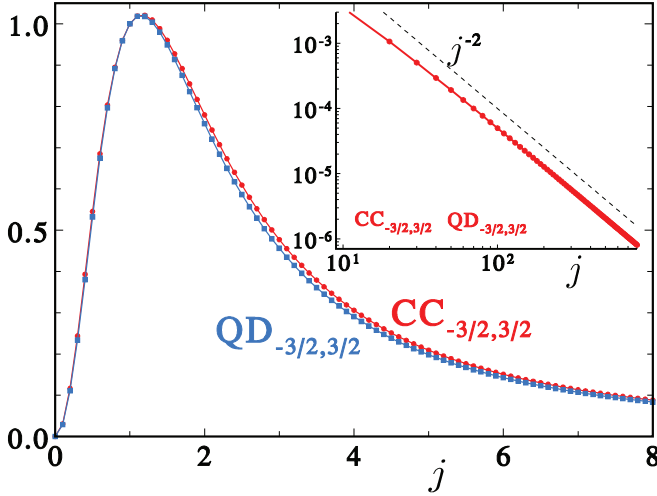


FIG. 4. (Color online) QD and CC (normalized with respect to the $j = 1$ value) plotted vs j for the two spins at sites $\pm 3/2$, i.e., sitting at opposite sides of the impurity. Cutting the chain affects both quantum and classical correlations in an essentially identical way. Inset: Log-log plot of QD and CC (here indistinguishable) vs j , showing that they obey a j^{-2} scaling law, which is in fact independent of the distance of the sites.

In order to provide an all-round characterization of our proposal, we now complement the analysis performed above by addressing the leakage of information out of head and tail of the segment effectively obtained by increasing j . We quantify the extent of such leakage by addressing the values taken by both classical correlations (CC) and quantum discord (QD) [20–22,27] across the impurity, i.e., between two spins sitting on opposite sides with respect to the BI, normalized by their respective values for $j = 1$.

The results corresponding to considering the spins at sites $n = \pm 3/2$ are shown in Fig. 4. Both CC and QD across the BI are nonmonotonic functions of the strength j . For small values of j , both rapidly grow. On the other hand, the range $j \gg 1$ corresponds to the monotonic decrease of all forms of correlations, thus demonstrating that the ring is effectively cut. Remarkably, for $j \gtrsim 1$, CC and QD are larger than their value at $j = 1$. This is due to the spread of the localized state over these sites, yielding an enhancement similar to that reported in Refs. [15,16,18], to which we refer for a detailed discussion. CC and QD behave in very similar ways, decaying asymptotically, for $j \gg 1$, as j^{-2} (cf. the inset of Fig. 4). This power-law decay stems from the behavior of the magnetic correlations. In fact, these enter both the expression of the concurrence [cf. Eq. (9) below] and those of QD and CC (which are not reported here as too lengthy to be informative). In particular, by considering Eqs. (5) and (6) in the $j \gg 1$ limit, and evaluating by standard methods the magnetic correlation functions (as done, for instance, in Ref. [24]), we find that $\langle \hat{\sigma}_n^x \hat{\sigma}_m^x \rangle = O(j^{-(|n|+|m|)})$, whereas $\langle \hat{\sigma}_n^z \hat{\sigma}_m^z \rangle = O(j^{-2})$, regardless of the relative distance between the spins. As a consequence, the scaling law j^{-2} reported in the inset of Fig. 4 originates from the correlations along the z axis and is thus independent of the site separation. On the contrary, the correlation functions along the x axis shown in Fig. 3(a) do depend on the distance, as reported above.

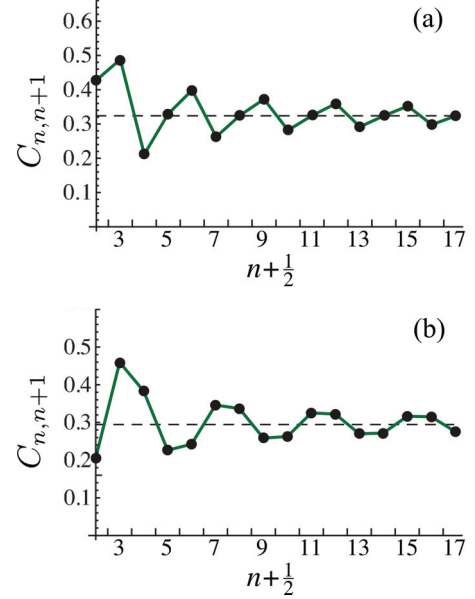


FIG. 5. (Color online) Nearest-neighbor concurrence $C_{n,n+1}$ for $j = 6$ vs the bond index $n + \frac{1}{2}$. Panels (a) and (b) are for $h = 0.5$, $\frac{1}{\sqrt{2}}$ respectively. The straight dashed line shows the value of the concurrence at $j = 1$. The magnetic field sets the periodicity of the one- and two-point spin correlators, which enter the concurrence, to $p = 3, 4$ respectively.

We conclude this section by briefly discussing how, by tuning the intensity of the impurity strength, it is possible to exploit the Friedel oscillations in order to spatially modulate the concurrence [28] between neighboring spins. In Fig. 5 we show the nearest-neighbor concurrence for $j = 6$ at different values of h . Analytically, the concurrence $C_{n,m}$ depends on the magnetic correlation functions as [29]

$$C_{n,m} = \max \left[0, \langle \hat{\sigma}_n^x \otimes \hat{\sigma}_m^x \rangle - \frac{1}{2} \sqrt{(S_{nm}^{zz})^2 - (s_{nm}^{zz})^2} \right], \quad (9)$$

with $S_{nm}^{zz} = 1 \pm \langle \hat{\sigma}_n^z \otimes \hat{\sigma}_m^z \rangle$ and $s_{nm}^{zz} = \langle \hat{\sigma}_n^z \rangle + \langle \hat{\sigma}_m^z \rangle$. The values of $C_{n,m}$ achieved in our system are the same as those of an open-boundary spin chain in the presence of a strong magnetic field on a single spin [16,30]. Moreover, we notice the presence of a periodic spatial modulation (with respect to the value of concurrence achieved for PBC), determined by the periodicity $p = \pi / \cos^{-1} h$ of the Friedel oscillations, as reported also for different impurity types in Refs. [15,17].

IV. EFFECTIVE RING-CUTTING MECHANISM: ANALYSIS OF THE STATE FIDELITY

In order to further verify the efficiency of the proposed mechanism, we now take a different point of view and consider a global figure of merit from which we can obtain indications on the similarity between the state of the cut ring and that of a true segment. As a description of the state of the former, we choose the reduced density matrix $\rho = \text{Tr}_{n=\pm \frac{1}{2}} [|\Omega\rangle\langle\Omega|]$ of a $2(M-1)$ spin system where the impurity spins have been traced out of the ring. As for the state of a segment, which embodies our target state, we take the pure state $|\Sigma\rangle$ of a system of $2(M-1)$ spins with OBC. As a measure of

closeness between two quantum states we use the quantum fidelity [23] $\mathcal{F}(|\Sigma\rangle, \rho) = \langle \Sigma | \rho | \Sigma \rangle$.

The ground state of a free-fermion model such as the one in Eq. (3) is given by

$$|\Omega\rangle = \prod_{k: E_k < 0} \hat{\xi}_k^\dagger |0\rangle, \quad (10)$$

for which all the negative-energy eigenstates up to the Fermi energy $E_{k_F} = 0$ are occupied by a fermionic quasiparticle, whereas positive-energy levels are empty. As a consequence, states with a different number of fermions yield zero fidelity. As the number of fermions in the Dirac sea is given by the intensity of the magnetic field h , which sets the Fermi momentum, we will compare the actual state of the cut ring with a target state for the same value of the applied magnetic field. A somewhat lengthy but otherwise straightforward calculation based on the use of Wick's theorem shows that \mathcal{F} depends on the submatrices of the transformation mapping the real-space fermions \hat{c}_n to those diagonalizing the Hamiltonian in the case of Eq. (4) (the target model) for $n = -M+1/2, \dots, M-1/2$ and $k < k_F$. Some details of this derivation are sketched in Appendix B.

In Fig. 6 the fidelity is shown as a function of $j > 1$ for different values of h and M . As a perturbative analysis suggests, for $j \gg 1$ the ground state of our model tends to the factorized state $|\Psi^+\rangle_{\pm\frac{1}{2}} \otimes |\omega\rangle_{-\frac{3}{2}, \dots, \frac{3}{2}}$, where $|\Psi^+\rangle_{\pm\frac{1}{2}}$ is a Bell state of the spins across the BI, while $|\omega\rangle_{-\frac{3}{2}, \dots, \frac{3}{2}}$ is a pure state of the rest of the system. Figure 6 shows that, almost independently of the magnetic field value, the mixed state of the reduced system is almost indistinguishable from the target state for relatively small values of the impurity strength. As far as finite-size effects are involved, we note that the shorter the ring, the lower the value of j needed for cutting it, although differences decrease with increasing j and h [see Figs. 6(a)–6(c)]. On the other hand, for $h \geq 1$ finite-size effects are almost absent but for $j \lesssim 2$ [cf. Fig. 6(d)]. This can be easily explained by noticing that the target state is fully polarized, $|\Sigma\rangle = |0\rangle^{\otimes 2(M-1)}$, while the ground state of the ring is $|\Omega\rangle = \hat{\xi}_-^\dagger |0\rangle$. When the localization length q^{-1} is less than the length of the ring $2M$, by taking into account Eq. (7) we get that the spins located at a distance $d > q^{-1}$ are, for all practical purposes, in state $|0\rangle$. As a consequence, considering longer chains will not affect substantially the value of the fidelity due to the presence in the ground state of our model of only a single localized mode. This is at variance with the case $h < 1$ where the extended (distorted) eigenstates given by Eq. (5), spread all over the chain. Therefore, for $h \geq 1$ the length of the ring does not play a significant role. Moreover, the analytical expression for the fidelity in the thermodynamic limit reads $\mathcal{F} = 1 - e^{-2q} = 1 - 1/j^2$. It is worth noticing that, for all practical purposes, the thermodynamic limit is already reached when the length of the chain exceeds the localization length $q^{-1} = 1/(\ln j)$. Finally, for arbitrarily large values of h , the target state does not change because the XX Heisenberg model enters the saturated phase. In addition, as the localized mode is independent of h , the ground state of our model is invariant for $h \geq 1$. This yields the very same behavior of the fidelity for $h > 1$ as that reported in Fig. 6(d).

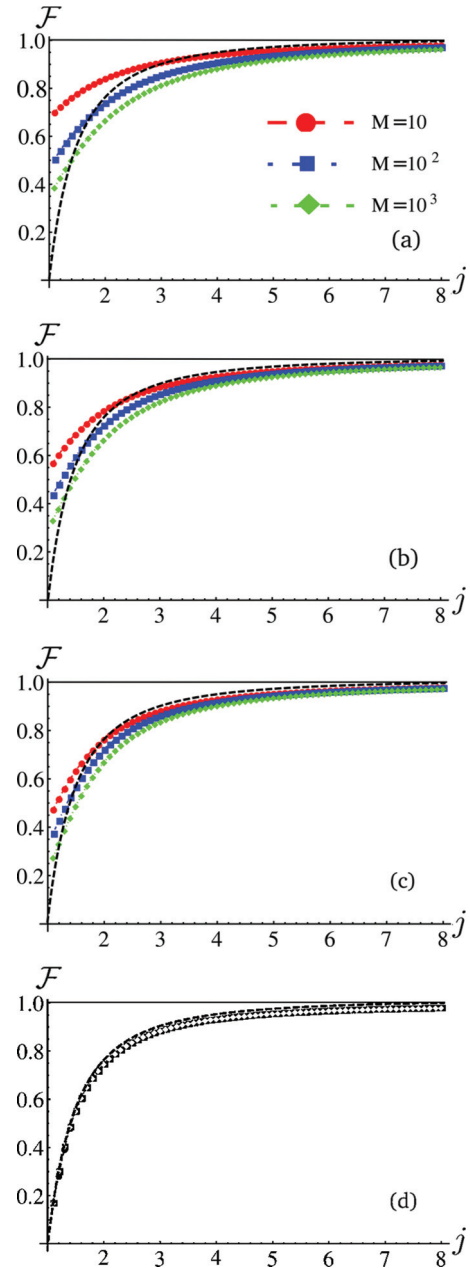


FIG. 6. (Color online) Fidelity $\mathcal{F}(|\Sigma\rangle, \rho)$ between the reduced state ρ of our model and the pure state $|\Sigma\rangle$ of a linear chain with the same number of spins by varying the coupling strength $j > 1$ at different values of the magnetic field $h = 0, \frac{1}{2}, \frac{1}{\sqrt{2}}, 1$ [panels (a), (b), (c), and (d) respectively]. We have taken $M = 10, 100, 1000$ in all panels. The dashed line shows the behavior of the function $1 - 1/j^2$, which matches the thermodynamic limit of the state fidelity at large magnetic fields.

V. CONCLUSIONS

We have shown that, by means of a BI, it is possible to turn a spin chain with PBC into an open boundary one. The XX impurity model has been solved analytically in the thermodynamical limit and two-points magnetic correlations functions, as well as CC and QD, have been shown to decay to zero for spin residing across the BI already for a relatively modest value of the impurity strength. The analogous figures

of merit for pairs of spins residing on the same side of the BI take values approaching those of a chain with OBC. For finite, yet arbitrarily large, spin chains, the fidelity between the ground state of a chain including all the spins but those coupled by the BI and an open chain of the same size, has been adopted in order to confirm the validity of the approach discussed here. It follows that impurity bonds can be used in otherwise translation-invariant systems as a means to achieve an effective cutting of the spin chain at the desired point. The full analytical treatment provided here allows for an exact quantification of the cutting quality.

This result shows the possibility, via impurity bonds, to break up physical systems with a ring topology or to cut long chains in smaller ones by different specific techniques depending on the actual physical implementation, such as chemical doping in molecular spin arrays [4,5], site-dependent modulation of the trapping laser in cold atoms or ions systems [6], or spatial displacement of an optical cavity in an array [7]. This could be exploited in order to make some systems more useful for quantum-state transfer, where often a necessary requisite consists in an addressable head and tail as well as in the finiteness of the quantum data bus. Finally, tuning the values of the impurity strength within $j \in [0, 10]$ is sufficient to investigate the emergence of edge effects, such as total or partial wave function backscattering which, by choosing an appropriate uniform magnetic field, spatially modulate the spin correlations functions.

ACKNOWLEDGMENTS

T.J.G.A. is supported by the European Commission, the European Social Fund and the Region Calabria through the program POR Calabria FSE 2007-2013–Asse IV Capitale Umano-Obiettivo Operativo M2. L.B. is supported by the ERC Grant No. PACOMANEDIA. M.P. thanks the Alexander von Humboldt Stiftung, the UK EPSRC for a Career Acceleration Fellowship, the “New Directions for EPSRC Research Leaders” initiative (Grant No. EP/G004759/1), and the John Templeton Foundation (Grant No. 43467).

APPENDIX A: DIAGONALIZATION OF THE HAMILTONIAN

We introduce the $2M$ discretized wave vectors $k \equiv \pi \ell / M$ ($\ell = -M+1, \dots, M$) and the fermionic operators

$$\hat{c}_k = \frac{1}{\sqrt{2M}} \sum_n e^{ink} \hat{c}_n, \quad (\text{A1})$$

corresponding to excitations of energy $E_k = 2(\cos k - h)$. States with one fermionic excitation of (unperturbed) energy E_k are $|k\rangle = \hat{c}_k^\dagger |0\rangle$, where $|0\rangle$ is the fermionic vacuum state. In this appendix, the analysis is restricted to the single particle sector of the full Fock state, spanned by these states. Due to the noninteracting form of the Hamiltonian, the diagonalization performed in this one-particle sector allows us to straightforwardly obtain the full many-fermion energy eigenstates. The Green operator of the unperturbed (one-particle) Hamiltonian

is thus defined as

$$\hat{G}_0(z) = \frac{1}{z - \hat{\mathcal{H}}_0} = \sum_k \frac{1}{z - E_k} |k\rangle \langle k| \quad (z \in \mathbb{C}). \quad (\text{A2})$$

In the thermodynamic limit ($M \rightarrow \infty$), the summation is changed into an integral and the discrete energies E_k become a continuous energy band. The matrix elements of the Green operator in the lattice position space read

$$G_0(n, m; z) = \frac{(-x + \sqrt{x^2 - 1})^{|n-m|}}{2\sqrt{x^2 - 1}} \quad \text{for } z \notin I_b, \quad (\text{A3})$$

$$G_0^\pm(n, m; z) = \frac{(-x \pm i\sqrt{1-x^2})^{|n-m|}}{\pm 2i\sqrt{1-x^2}} \quad \text{for } z \in I_b,$$

where $x = z/2 + h$, while $I_b = [-2h-2, -2h+2]$ is the unperturbed energy band. The Green operator $\hat{G}(z)$ associated with the (one-particle restriction of) the Hamiltonian in Eq. (3) can be now obtained by the relation $\hat{G}(z) = \hat{G}_0(z) + \hat{G}_0(z) \hat{T}(z) \hat{G}_0(z)$, where the matrix $\hat{T}(z) = (\sum_{l=0}^{\infty} [\hat{\mathcal{H}}_1 \hat{G}_0(z)]^l) \hat{\mathcal{H}}_1$ can be analytically summed up to all terms. Finally, the knowledge of $\hat{G}(z)$ allows us to obtain the whole (single-particle) spectrum of the Hamiltonian, which consists of the above-mentioned energy band and a pair of out-of-band discrete energy eigenstates, which are simple poles of $\hat{G}(z)$ appearing only for $j > 1$. In order to obtain the corresponding eigenstates, we use the relation $|\Psi_E\rangle = [\mathbb{1} + \hat{G}_0^+(E) \hat{T}^+(E)] |k\rangle$ for the continuous in-band states, which describe distorted spin waves of the system that are built from the unperturbed ones by including the corrections due to the scattering from the defect and described by the retarded Green operator $\hat{G}_0^+(z)$ and the $\hat{T}(z)$ operator. The Schrödinger equation of the full problem is then solved by using an appropriate Ansatz for the two discrete out-of-band energy eigenstates [26].

APPENDIX B: RING CUT FIDELITY

The ring cut fidelity is easily obtained from the explicit expression of the ground states (10). In order to elucidate the main steps of this derivation let us consider two sets of Fermi operators $\hat{\chi}_k = \sum_n V_{kn} \hat{c}_n$, $\hat{\xi}_k = \sum_n U_{kn} \hat{c}_n$. The fidelity between two *Dirac seas* follows then from Wick's theorem,

$$\langle 0 | \prod_{k=1}^{K_F} \chi_k \prod_{k'=1}^{K_{F'}} \xi_{k'}^\dagger | 0 \rangle = \begin{cases} 0 & \text{if } K_F \neq K_{F'} \\ \det G & \text{if } K_F = K_{F'} \end{cases}, \quad (\text{B1})$$

$$G_{kk'} = \langle 0 | \chi_k \xi_{k'}^\dagger | 0 \rangle = \sum_n V_{kn} U_{k'n}^*. \quad (\text{B2})$$

The ring cutting fidelity then reads

$$F = \langle \Sigma | \text{Tr}_{n=\pm\frac{1}{2}} [|\Omega\rangle \langle \Omega|] | \Sigma \rangle$$

$$= |\langle \tilde{\Sigma} | \Omega \rangle|^2 + |\langle \tilde{\Sigma} | c_{-\frac{1}{2}} | \Omega \rangle|^2$$

$$+ |\langle \tilde{\Sigma} | c_{+\frac{1}{2}} | \Omega \rangle|^2 + |\langle \tilde{\Sigma} | c_{-\frac{1}{2}} c_{+\frac{1}{2}} | \Omega \rangle|^2, \quad (\text{B3})$$

where $|\tilde{\Sigma}\rangle$ refers to the state $|\Sigma\rangle$ extended to the larger Fock space of $2M$ Fermions. Each term of the above sum is then evaluated from (B1) with a suitable choice of the matrices V and U .

- [1] For reviews see S. Bose, *Contemp. Phys.* **48**, 13 (2007); T. J. G. Apollaro, S. Lorenzo, and F. Plastina, *Int. J. Mod. Phys. B* **27**, 1345305 (2013).
- [2] M. Christandl, N. Datta, A. Ekert, and A. J. Landahl, *Phys. Rev. Lett.* **92**, 187902 (2004); T. J. G. Apollaro, L. Banchi, A. Cuccoli, R. Vaia, and P. Verrucchi, *Phys. Rev. A* **85**, 052319 (2012); A. Ajoy and P. Cappellaro, *Phys. Rev. B* **87**, 064303 (2013); T. Linneweber, J. Stolze, and G. S. Uhrig, *Int. J. Quantum Inf.* **10**, 1250029 (2012); L. Banchi, A. Bayat, P. Verrucchi, and S. Bose, *Phys. Rev. Lett.* **106**, 140501 (2011); L. Banchi, arXiv:1309.0069 (2013); S. Lorenzo, T. J. G. Apollaro, A. Sindona, and F. Plastina, *Phys. Rev. A* **87**, 042313 (2013).
- [3] H. J. Mikeska and M. Steiner, *Adv. Phys.* **40**, 191 (1991).
- [4] G. A. Timco *et al.*, *Nat. Nanotechnol.* **4**, 173 (2009).
- [5] F. Troiani, V. Bellini, A. Candini, G. Lorusso, and M. Affronte, *Nanotechnology* **21**, 274009 (2010).
- [6] M. Lewenstein, A. Sanpera, and V. Ahufinger, *Ultra-Cold Atoms in Optical Lattices: Simulating Quantum Many-Body Systems* (Oxford University Press, Oxford, 2012).
- [7] S. M. Giampaolo and F. Illuminati, *New J. Phys.* **12**, 025019 (2010).
- [8] S. Eggert and I. Affleck, *Phys. Rev. B* **46**, 10866 (1992).
- [9] S. Rommer and S. Eggert, *Phys. Rev. B* **62**, 4370 (2000).
- [10] C. Schuster and U. Eckern, *Ann. Phys.* **11**, 901 (2002).
- [11] J. Friedel, *Nuovo Cimento Suppl.* **7**, 287 (1958).
- [12] G. Baskaran, *Phys. Rev. Lett.* **40**, 1521 (1978).
- [13] G. Gildenblat, *J. Magn. Magn. Mater.* **43**, 96 (1984); *Phys. Rev. B* **32**, 3006 (1985); **47**, 2611 (1993).
- [14] S. Shinkevich, O. F. Syljuåsen, and S. Eggert, *Phys. Rev. B* **83**, 054423 (2011).
- [15] O. Osenda, Z. Huang, and S. Kais, *Phys. Rev. A* **67**, 062321 (2003).
- [16] T. J. G. Apollaro, A. Cuccoli, A. Fubini, F. Plastina, and P. Verrucchi, *Phys. Rev. A* **77**, 062314 (2008).
- [17] T. J. G. Apollaro *et al.*, *Int. J. Quantum Inf.* **6**, 567 (2008).
- [18] F. Plastina and T. J. G. Apollaro, *Phys. Rev. Lett.* **99**, 177210 (2007).
- [19] W. K. Wootters, *Phys. Rev. Lett.* **80**, 2245 (1998).
- [20] H. Ollivier and W. H. Zurek, *Phys. Rev. Lett.* **88**, 017901 (2001).
- [21] L. Henderson and V. Vedral, *J. Phys. A* **34**, 6899 (2001).
- [22] K. Modi, A. Brodutch, H. Cable, T. Paterek, and V. Vedral, *Rev. Mod. Phys.* **84**, 1655 (2012).
- [23] R. Jozsa, *J. Mod. Opt.* **41**, 2315 (1994).
- [24] E. Lieb, T. Schultz, and D. Mattis, *Ann. Phys.* **16**, 407 (1961).
- [25] E. N. Economou, *Green Functions in Quantum Physics* (Springer Verlag, Berlin, 1983).
- [26] P. A. Pury and S. A. Cannas, *J. Phys. A* **24**, L1405 (1991).
- [27] In this manuscript we adopt the entropic definition of discord given in Ref. [20]. Thanks to the symmetries of the density matrix describing the state of the spins across the BI, exact analytical expressions for such figure of merit can be obtained [31].
- [28] C. H. Bennett, D. P. Di Vincenzo, J. A. Smolin, and W. K. Wootters, *Phys. Rev. A* **54**, 3824 (1996).
- [29] A. Fubini, T. Roscilde, V. Tognetti, M. Tusa, and P. Verrucchi, *Eur. Phys. J. D* **38**, 563 (2006).
- [30] W. Son, L. Amico, F. Plastina, and V. Vedral, *Phys. Rev. A* **79**, 022302 (2009).
- [31] S. Luo, *Phys. Rev. A* **77**, 042303 (2008).